Journal of Oceanography, Vol. 65, pp. 151 to 164, 2009

Seasonal and Interannual Variation of North Pacific Subtropical Mode Water in 2003–2006

Eitarou Oka*

Ocean Research Institute, The University of Tokyo, Nakano-ku, Tokyo 164-8639, Japan

(Received 16 October 2007; in revised form 1 May 2008; accepted 8 September 2008)

Temperature and salinity data from 2003 through 2006 from Argo profiling floats have been analyzed to examine the formation and circulation of the North Pacific Subtropical Mode Water (STMW) and the interannual variation of its properties over the entire distribution region. STMW is formed in late winter in the zonally-elongated recirculation gyre south of the Kuroshio and its extension, which extends north of ~28°N, from 135°E to near the date line. The recirculation gyre consists of several anticyclonic circulations, in each of which thick STMW with a characteristic temperature is formed. After spring, the thick STMW tends to be continually trapped in the respective circulations, remaining in the formation region. From this stagnant pool of thick STMW, some portion seeps little by little into the southern region, where southwestward subsurface currents advect relatively thin STMW as far as 20°N to the south and just east of Taiwan to the west. The STMW formed in the recirculation gyre becomes colder, less saline, and denser to the east, with an abrupt change of properties across 140°E and a gradual change east of 140°E. The STMW formed east of 140°E exhibits coherent interannual variations, increasing its temperature by ~1°C from 2003 through 2006 and also increasing its salinity by ~0.05 from 2003 through 2005. These property changes are clearly detected in the southern region as far downstream as just east of Taiwan, with reasonable time lags.

Keywords:
· North Pacific Subtropical Mode Water,
· seasonal variation,
· interannual variation,
· Argo.

1. Introduction

North Pacific Subtropical Mode Water (STMW; Masuzawa, 1969) is identified as a thermostad of 16°–19°C within or near the top of the permanent thermocline in the northwestern North Pacific subtropical gyre (Hanawa and Talley, 2001). Its name derives from the fact that it produces a mode in the volume distribution on the temperature–salinity diagram for the subtropical gyre.

The formation and circulation of STMW were examined intensively from the late 1980s through the 1990s, during which a fundamental view was established. Specifically, a deep mixed layer is formed in late winter just south of the Kuroshio and the Kuroshio Extension (KE), where warm water supplied from the Kuroshio/KE and strong winter monsoon from the Asian continent lead to a large heat loss from the ocean to the atmosphere (Hanawa, 1987; Suga and Hanawa, 1990; Bingham, 1992). The developed mixed layer, STMW, is capped by the seasonal thermocline in spring, and then transported by the southwestward Kuroshio recirculation to spread over the northwestern subtropical gyre (Bingham, 1992; Suga and Hanawa, 1995a).

Several studies have demonstrated that the amount and properties of STMW formed each winter are related to the intensity of the winter monsoon, represented by the sea level pressure difference between Nemuro, Japan and Irkutsk, Russia. That is, thicker and colder STMW tends to be formed in winters with strong monsoon (Suga and Hanawa, 1995b; Yasuda and Hanawa, 1999; Taneda *et al*., 2000; Hanawa and Kamada, 2001; Hanawa and Yoritaka, 2001), a relation that also applies to the subtropical mode water in the North Atlantic (Kwon and Riser, 2004). Therefore, through its formation process, STMW is believed to transmit atmospheric conditions to the ocean subsurface every winter, in the form of temperature anomalies. In subsequent winters, such temperature anomalies might reappear at the sea surface in the same formation region or in a remote area, affecting sea surface temperature there. It is thus expected that STMW plays some role in regional climate variability, although it was difficult to examine the role in the 1990s and earlier, when only climatological data and a limited number of long time-series data were available.

* E-mail address: eoka@ori.u-tokyo.ac.jp

In 2000, profiling floats deployed in the international Argo project (Argo Science Team, 2001) started measuring temperature and salinity profiles down to 2000 dbar depth at 10 day intervals. These data, increasing in number year by year, made it possible to take snapshots of STMW at any time of a year, providing new perspectives on the STMW circulation. For example, the float data in February and March 2003 demonstrated that the STMW formation region, i.e., the deep mixed layer just south of the Kuroshio/KE, extends as far east as 175°E, which is much farther than previous studies had recognized (Oka and Suga, 2003). This indicates that the previous studies were only able to investigate the western portion of the STMW circulation, due to data limitations.

Uehara *et al*. (2003) analyzed early float data obtained southeast of Japan in 2001, and suggested that STMW is preferentially formed and transported in anticyclonic eddies prevailing in the Kuroshio recirculation region. The effects of mesoscale eddies on STMW variation were also addressed by Qiu and Chen (2006), who used available temperature data and altimetric sea surface height data during 1993–2004 to demonstrate that the formation rate of STMW south of Japan is controlled primarily by the dynamic state of the KE rather than the atmospheric forcing. That is, the KE path adopts a relatively stable state and a variable state alternately on interannual time scales, and less STMW is formed in the latter state because the associated high regional eddy activity promotes input of high potential-vorticity KE water to the south of the KE, disturbing the development of deep winter mixed layer there. Supporting this idea, Qiu *et al*. (2007) used float data southeast of Japan to indicate that the low-potential vorticity signature of STMW formed in late winter 2005 was weaker than in 2004, associated with a transition of the KE from the low eddy activity mode to the high eddy activity one.

Another observed fact that might be related to the STMW circulation is a significant positive correlation between winter sea surface temperature anomaly southeast of Japan and that around 30°N east of the date line one year later (Sugimoto and Hanawa, 2005). According to Sugimoto and Hanawa (2005), this correlation arises because part of STMW formed southeast of Japan is advected eastward by the KE in one year, transporting sea surface temperature anomaly. Such advection might be possible because the northern limit of STMW lies within the rapid eastward flow of the KE (Qiu *et al*., 2006), although it would be opposite to the southwestward STMW advection that has been commonly accepted.

These recent findings indicate the need for a detailed examination of the circulation and interannual changes of STMW through the entire distribution region using observed data obtained in situ. Fortunately, the Argo float network over the northwestern North Pacific subtropical gyre has steadily improved since 2000, particularly thanks to the intensive deployment of 20 floats in April–June 2004 and 28 floats in May–July 2005 southeast of Japan under the Kuroshio Extension System Study (KESS) program (Qiu *et al*., 2006, 2007) contributing to Argo. In 2006, after the KESS floats scattered over a wide region, we obtained an unprecedented float network performing relatively uniform, high-density observations over the northwestern subtropical gyre (see Fig. 2 for the distribution of float observations). Using the float data in 2006, we here re-examine the seasonal evolution of STMW and its relation to the subsurface flow field south of the Kuroshio/KE. We also examine the interannual variation of STMW properties using the 2003–06 data, and investigate how the advection of STMW transports temperature and salinity anomalies to the downstream region.

2. Data

We used temperature (T) and salinity (S) data obtained by Argo profiling floats in the North Pacific in 2003–2006. These floats drift freely at a predetermined parking pressure (typically 1000 dbar), and ascend to the sea surface conducting T–S measurements at a predetermined interval (10 days) after descending to the maximum pressure (2000 dbar). Since the parking pressure of most floats is much deeper than the STMW depth range (typically shallower than 400 dbar), we assume here that the floats visit a different water parcel in the STMW depth range in every ascent. In other words, we assume that each float observation of STMW is independent.

The real-time quality controlled float data were downloaded from the ftp site of Argo Global Data Assembly Center (ftp://usgodae1.fnmoc.navy.mil/pub/outgoing/argo, ftp://ftp.ifremer.fr/ifremer/argo). From these data, defective T–S profiles, such as those with measurements flagged as bad and those lacking intermediate layers for certain depths, were eliminated, following the procedures of Oka *et al*. (2007). For 2003 and 2004, quarterly T–S data along the 137°E meridian collected by Japan Meteorological Agency (2005, 2006) using a shipboard conductivity-temperature-depth profiler were added to fill data gaps south of Japan. After each T–S profile was interpolated on a 1-dbar grid using the Akima spline (Akima, 1970), potential temperature (θ), potential density (σ_θ), and potential vorticity (Q) were calculated. Here, Q is defined as

$$Q = -\frac{f}{\rho}\frac{\partial \sigma_\theta}{\partial z}, \tag{1}$$

where f is the Coriolis parameter, ρ in-situ water density, and z is the vertical coordinate (positive upward). In Eq. (1), relative vorticity is neglected because it is much

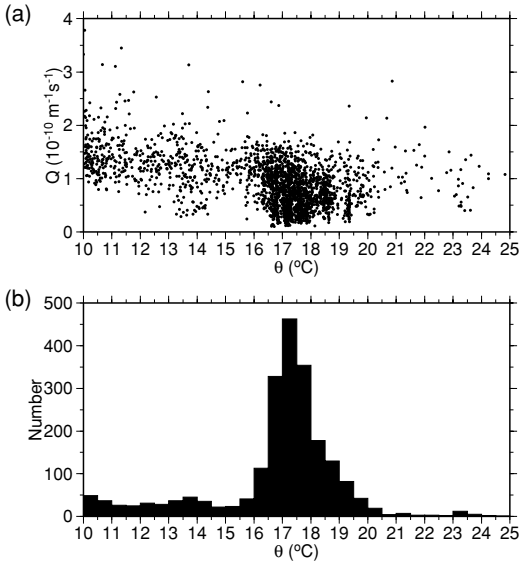

Fig. 1. (a) Plots of Q against θ at the Q minimum in each profile at 20°–35°N, 130°–165°E in April–June of 2003–2006. The Q minimum was chosen in a θ range of 10°–25°C. (b) Number of plots in (a) with $Q < 1.5 \times 10^{-10}$ m^{-1}s^{-1}, classified in each 0.5° bin of θ.

smaller than planetary vorticity except in the vicinity of the Kuroshio/KE axis (Qiu *et al*., 2006).

We also used delayed-time sea surface height data merged from TOPEX/Poseidon, Jason, ERS-1/2, and Envisat altimeter observations, produced by Ssalto/Duacs and distributed by AVISO (Ducet *et al*., 2000). The weekly data in 2003–2006, provided on a 0.25° × 0.25° grid, were downloaded from the web site of AVISO (http://www.aviso.oceanobs.com). The sea surface height maps for one, two, or three months presented in the latter sections were constructed by averaging the original weekly data.

3. Definition of STMW

Since STMW is characterized by vertical homogeneity, previous studies have defined it as a portion of a vertical profile with Q lower than a certain value. This critical value may be chosen arbitrarily, and values of ~2×10^{-10} m^{-1}s^{-1} have been employed by many studies using climatologies (e.g., Suga and Hanawa, 1995a; Suga *et al*., 2004) or bottle data (e.g., Suga *et al*., 1989; Suga and Hanawa, 1995b). In this study, we adopt a smaller value of 1.5×10^{-10} m^{-1}s^{-1}, which is the same value as that used by Uehara *et al*. (2003) to define STMW in Argo profiles, taking advantage of float data with relatively high vertical resolution and without any averaging.

Within the low-Q portion of a profile, the core, defined by the Q minimum, is considered to be least modified since the low-Q portion was formed, thus best preserving the water properties at the time of formation. To determine a θ range for the STMW core, Q and θ at the core are plotted for all profiles in spring in the northwestern subtropical gyre (Fig. 1(a)). The core with $Q < 1.5 \times 10^{-10}$ m^{-1}s^{-1} exists over the whole θ range between 10° and 25°C, but the plots concentrate in a range between 16° and 19.5°C, showing an outstanding peak in the histogram of number of the plots (Fig. 1(b)). Although this peak is probably highly overestimated due to the uneven distribution of float observations, particularly associated with intense observations southeast of Japan by the KESS floats during 2004 and 2005 (Qiu *et al*., 2006, 2007), it implies that there is a greater volume of 16°–19.5°C water than colder or warmer water, producing a mode in the volume distribution on the θ–S diagram, as pointed out by Masuzawa (1969). We therefore define STMW in each profile as a layer of $Q < 1.5 \times 10^{-10}$ m^{-1}s^{-1} with the core θ between 16° and 19.5°C. The low-Q layers with thickness less than 25 dbar and those existing only at depths less than 100 dbar are regarded as small-scale features and are excluded. STMW is considered to outcrop at the sea surface if its top is located at a depth less than 10 dbar.

4. Seasonal Variation of STMW Structure in 2006

Figure 2 shows distributions of STMW thickness in two-month periods from January–February through November–December, 2006, superimposed on maps of geopotential anomaly at 250 dbar (average depth of the STMW core from spring through fall) relative to 950 dbar. Geopotential anomaly maps were drawn from the float data using an optimal interpolation technique (Bretherton *et al*., 1976), with the annual-mean geopotential anomaly distribution based on the World Ocean Atlas 2001 climatology (Conkright *et al*., 2002) as an initial estimate and a correlation function of the form:

$$C = 0.5e^{-(d/500)} + 0.5e^{-(d/150)^2}, \qquad (2)$$

where d is distance in kilometers. This function is similar in form to the one used by Roemmich *et al*. (2007), considering both large-scale variation and mesoscale variability in the subtropical North Pacific with a dominant scale length of ~150 km (Kuragano and Kamachi, 2000).

From January through April, STMW outcrops at the sea surface south of the Kuroshio/KE (the large southward gradient of geopotential anomaly at ~34°N). This outcropping area is regarded as the formation region of STMW in late winter 2006. The formation region extends zonally from 136°E to near the date line, as in late winter 2003 (Oka and Suga, 2003), and its southern end is located at 28°N west of 150°E and at 29°N east of 150°E,

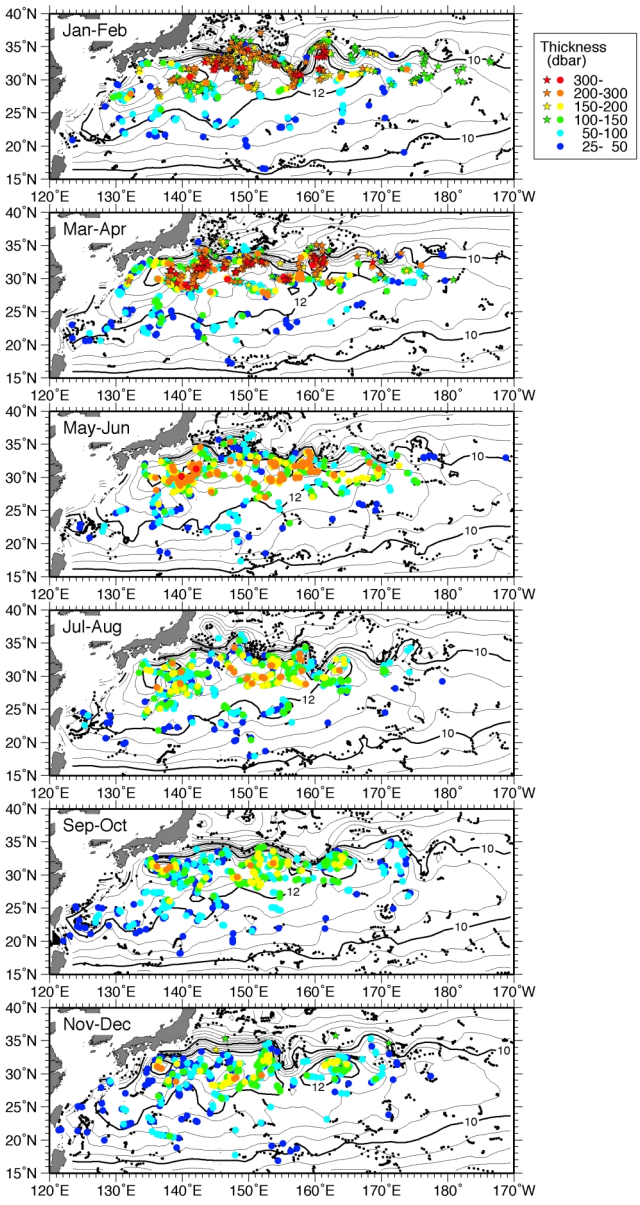

Fig. 2. Distributions of STMW thickness (dbar; stars and circles) and geopotential anomaly at 250 dbar relative to 950 dbar (m^2s^{-2}; contours) from January–February through November–December in 2006. Stars (circles) denote STMW outcropping (not outcropping) at the sea surface. Black dots represent float observation points without STMW. Contour interval for geopotential anomaly is 0.5 m^2s^{-2}, with thick contours at 10, 12, and 14 m^2s^{-2}.

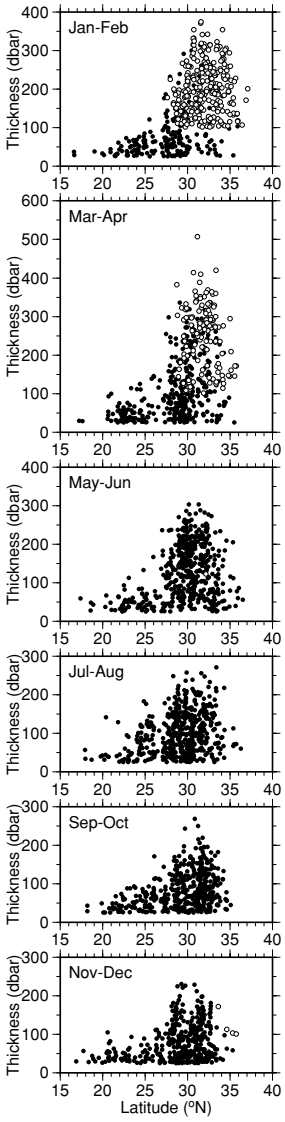

Fig. 3. Plots of STMW thickness against latitude from January–February through November–December in 2006. Open (closed) circles denote outcropping (non-outcropping) STMW.

shifting slightly northward toward the east. In the formation region, the STMW thickness exceeds 200 dbar west of 170°E, with the meridional maximum at 31°–32°N, a few degrees south of the KE (Fig. 3).

STMW does not outcrop south of 28°N (Fig. 2). The STMW observed there is supposed to be formed north of 28°N in previous winters and then advected southward across that latitude. The STMW south of 28°N lies in the southwestward subsurface current, being transported as far as 20°N to the south and just east of Taiwan to the west. It is thinner than 150 dbar, becoming thinner toward the south (Fig. 3). Consequently, the STMW thickness decreases sharply southward at the southern end of the formation region at 28°N. This latitude corresponds to that at which the winter mixed layer depth changes sharply (Fig. 4), a so-called mixed layer depth front that is theoretically important for the subduction of mode waters (Kubokawa and Inui, 1999; Kubokawa, 1999;

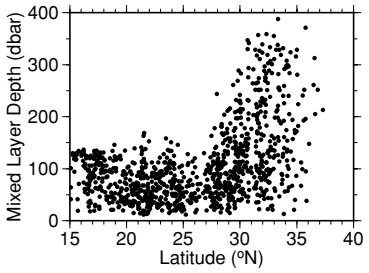

Fig. 4. Plots of mixed layer depth against latitude in February and March 2006. Plots were drawn only for profiles south of the Kuroshio Extension, judged by $\theta > 12$°C at 300 dbar (Mizuno and White, 1983). Mixed layer depth was defined as the depth at which σ_θ increases by 0.1 kg m^{-3} from 10-dbar depth.

Nishikawa and Kubokawa, 2007).

In May, the STMW north of 28°N stops outcropping, and thick STMW is left in the subsurface in almost the same location as the formation region in January–April (Fig. 2). This thick part is gradually eroded as the season progresses, while, in contrast to the traditional view, it shifts little in the meridional direction, maintaining its southern end at ~28°N until November–December (Fig. 3). The STMW south of 28°N remains relatively thin, except that STMW with a thickness of 100–200 dbar is temporarily advected from the formation region to 24°–26°N, 135°–140°E in July–August. As a result, the front of STMW thickness exists at ~28°N throughout the year.

The background contours of geopotential anomaly in Fig. 2 indicate that the region between 28°N and the Kuroshio/KE corresponds to the zonally-elongated anticyclonic recirculation gyre of the Kuroshio/KE (e.g., Kawai, 1972; Qiu, 2002; Qiu and Chen, 2005). This implies that after thick STMW is formed in the recirculation gyre in late winter, a large portion of it remains in the gyre until the end of the year, and a small portion leaves the gyre, entering the region south of 28°N where the flow is predominantly southwestward. The latter portion is so-called subducted, being expected to persist for years, while the former portion is likely to be re-entrained into the mixed layer developed in the recirculation gyre in the following winter.

It is worth noting that while the thick STMW is formed and circulates in the recirculation gyre, relatively thin SMTW with a thickness of several tens of decibars also exists there in a considerable amount (Figs. 2 and 3). This suggests that the STMW distribution is highly variable due to mesoscale disturbances, as demonstrated in a recent study using a high-resolution numerical model (Rainville *et al*., 2007).

How do the properties of the STMW formed in the recirculation gyre in late winter 2006 change zonally?

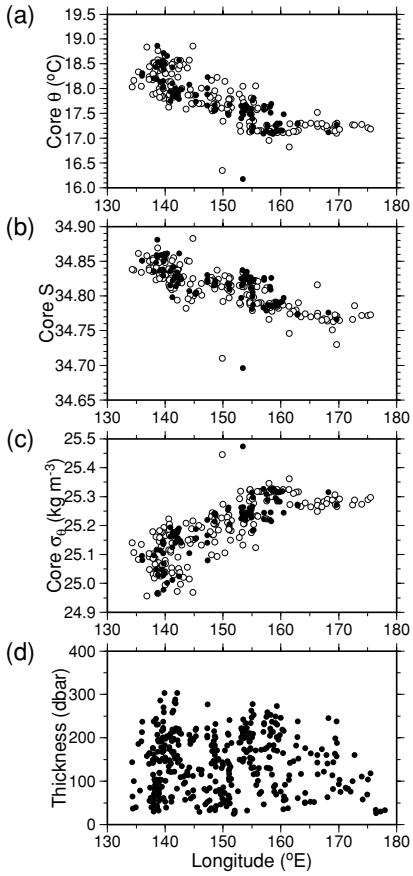

Fig. 5. Plots of (a) θ, (b) S, and (c) σ_θ at the core and (d) thickness of non-outcropping STMW north of 28°N against longitude in May and June 2006. Plots in (a)–(c) were drawn only for STMW thicker than 100 dbar, with closed (open) circles for STMW thicker than 200 dbar (with a thickness of 100–200 dbar).

Since the properties of outcropping STMW in winter are temporal ones during the formation process, properties at the core of non-outcropping STMW in May–June just after the formation period are presented in Fig. 5.

The core θ of STMW decreases toward the east, as demonstrated in previous studies (Suga and Hanawa, 1990; Bingham, 1992; Oka and Suga, 2003). It decreases sharply from 18.8°C to 17.8°C near 140°E, and more gradually east of 145°E, being almost uniform at ~17.2°C east of 160°E. The core S also decreases toward the east from 34.85 at 135°E to 34.77 at 170°E, due to the southward Ekman transport of less saline surface water north of the KE (Hanawa and Talley, 2001). The core σ_θ increases toward the east from 24.95 to 25.35 kg m^{-3}, reflecting mainly the eastward decrease of the core θ as large as 1.5°C, rather than that of the core S. The STMW thickness is at a maximum of 303 dbar at 140° and 142°E, decreasing gradually toward the east.

A further inspection of Fig. 5(a) reveals that the plots tend to be concentrated at particular core θ values, showing a step-like distribution. Indeed, the histogram of number of profiles having STMW in each core θ range exhibits three large peaks at 17.1°–17.3°C, 17.5°–17.7°C, and 17.8°–17.9°C and a smaller, broad peak at 17.9°–18.6°C adjacent to the third large peak (Fig. 6(a)). The thick STMW formed in late winter 2006 is thus classified into several "modes" according to the core θ.

Using these modes, we now examine the seasonal variation of STMW distribution in more detail. Figure 7 shows monthly distributions of three modes (17.1°–17.3°C, 17.5°–17.7°C, and 17.8°–18.6°C) of STMW from May through December 2006, superimposed on maps of geopotential anomaly at 250 dbar and altimetric sea surface height. Compared to the sea surface height maps, the geopotential anomaly ones constructed from the unevenly-distributed float data adequately capture the meandering path of the Kuroshio/KE and the southern recirculation gyre, except in some data-sparse regions. As demonstrated in previous studies (e.g., Kawai, 1972), the recirculation gyre consists of several anticyclonic circulations, most of which are associated with crests of the Kuroshio/KE meander.

These anticyclonic circulations are closely related to the distribution of each mode of STMW. In May, a large circulation exists at 134°–144°E, and four small circulations align to the east at 145°–149°E, 152°–155°E, 157°–160°E, and 167°–171°E. The 17.8°–18.6°C STMW thicker than 100 dbar mostly lies within the large circulation, the 17.5°–17.7°C one within the two western small circulations, and the 17.1°–17.3°C one within the two eastern small circulations. In the following months, the 17.1°–17.3°C and 17.5°–17.7°C STMW thicker than 100 dbar tends to be continually trapped in the respective circulations while the circulations gradually shift, occasionally merging/separating. Note that these anticyclonic circulations are relatively stagnant, compared to mesoscale eddies to the south which are propagating westward at a considerable speed (Ebuchi and Hanawa, 2001; also see, e.g., an anticyclonic eddy propagating along 25°N from 157°E in May to 142°E in December in the sea surface height maps in Fig. 7). Consequently, each mode of thick STMW trapped in the circulations does not migrate significantly in the zonal direction nor in the meridional direction. From these stagnant pools of thick STMW, some STMW parcels seep southward little by little, being subsequently transported southwestward.

In contrast with the 17.1°–17.3°C and 17.5°–17.7°C STMW, the 17.8°–18.6°C one tends to leave the western, large circulation. After spring, a large portion of the 17.8°–18.6°C STMW thicker than 100 dbar is discharged southward from the southeastern part of the large circulation near 135°–140°E, reaching 27°N in May and 24°N in July.

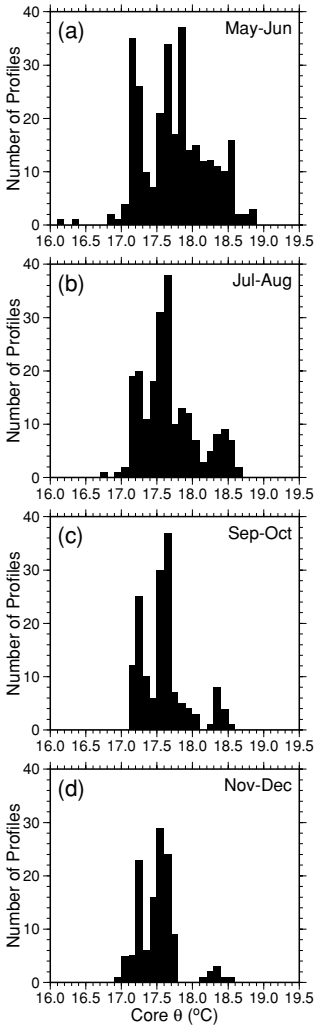

Fig. 6. Number of profiles with non-outcropping STMW thicker than 100 dbar in each 0.1° bin of core θ in (a) May–June, (b) July–August, (c) September–October, and (d) November–December of 2006.

The discharged portion then appears to lose its thickness quickly in the downstream region. These changes are reflected in the number of STMW thicker than 100 dbar with each core θ (Fig. 6). While the 17.1°–17.3°C and 17.5°–17.7°C STMW continues to be a mode until November–December, the 17.8°–18.6°C one rapidly decreases in number, almost disappearing in late fall.

It should be mentioned that some parcels of STMW, such as the 17.5°–17.7°C one at 34°N, 166°E in May, the 17.8°–18.6°C one at 32°N, 163°E in June, and the 17.5°–17.7°C one at 31°N, 171°E in July, are found in a much more easterly location than the other STMW parcels having the same core θ (Fig. 7). Since these remote parcels are located in the vicinity of the KE axis, they are likely to be transported eastward by the rapid flow of the KE.

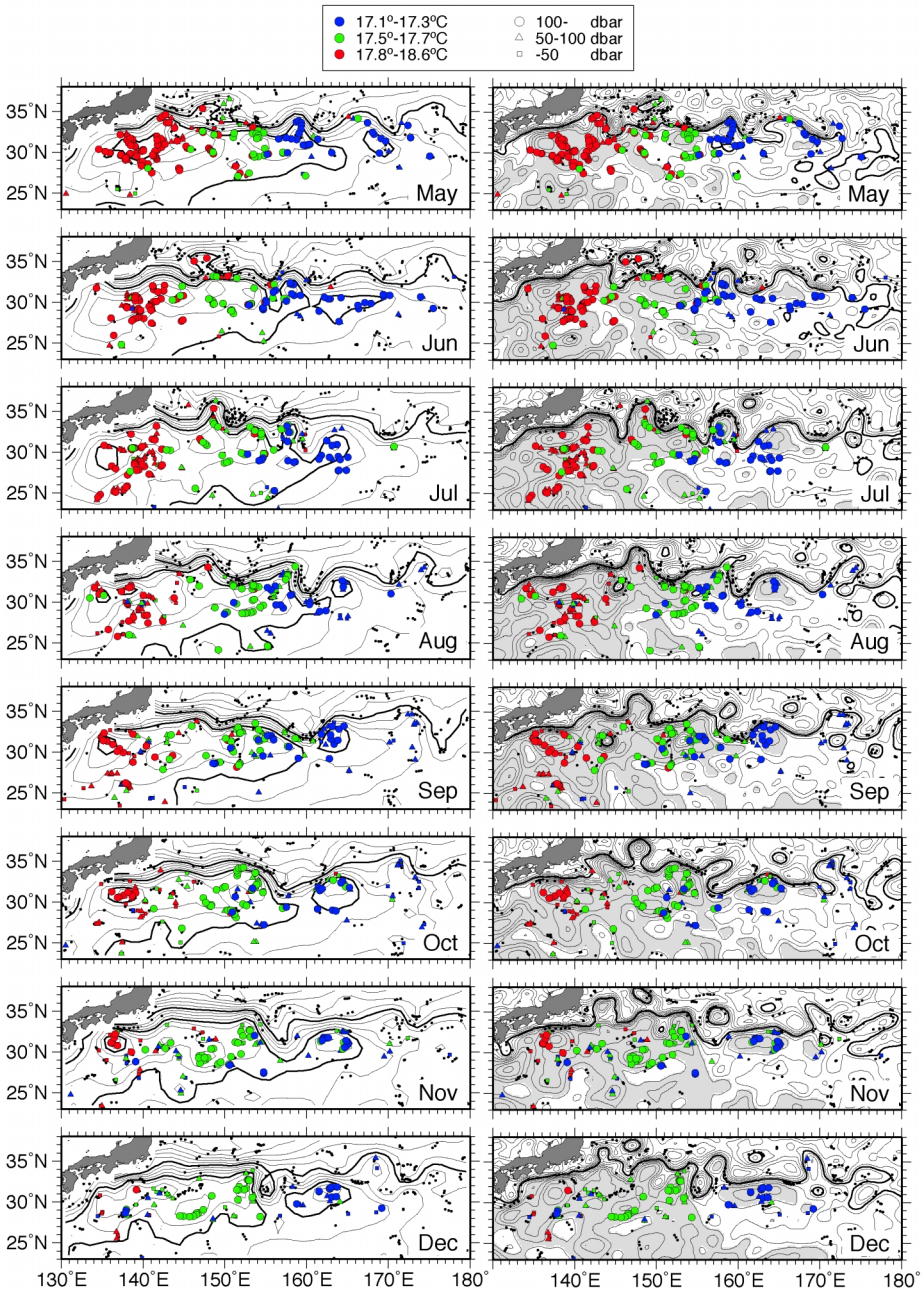

Fig. 7. Monthly distributions of SMTW with a core θ of 17.1°–17.3°C (blue symbols), 17.5°–17.7°C (green symbols), and 17.8°–18.6°C (red symbols) from May through December in 2006. The symbol type denotes STMW thickness: greater than 100 dbar (circles), 50–100 dbar (triangles), and less than 50 dbar (squares). Black dots denote float observation points with STMW having the other core θ and those without STMW. Background contours represent geopotential anomaly at 250 dbar relative to 950 dbar (left panels) and altimetric sea surface height (right panels). Contour for geopotential anomaly is drawn at an interval of 0.5 m^2s^{-2}, with thick ones at 10, 12, and 14 m^2s^{-2}. Contour for sea surface height is drawn at an interval of 10 cm, with a thick one at 220 cm and a shaded region for higher than 250 cm.

These transports, though low in number, might be related to the close correlation between winter sea surface temperature anomaly in the STMW formation region and that east of the date line one year later, indicated by Sugimoto and Hanawa (2005).

The anticyclonic circulations in the recirculation gyre are important not only for the circulation of each mode of STMW after spring but probably also for its forma-

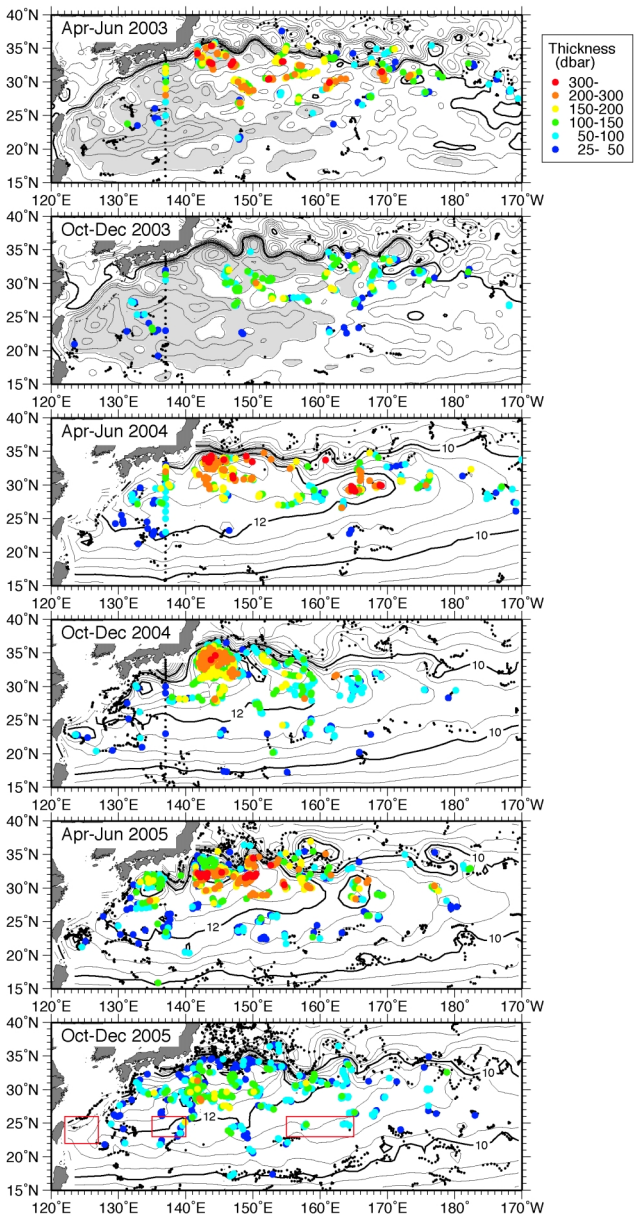

Fig. 8. Distributions of thickness of non-outcropping STMW (dbar; circles) in April–June and October–December of 2003–2005. Black dots represent float observation points without STMW. Background contours denote altimetric sea surface height (for 2003) and geopotential anomaly at 250 dbar relative to 950 dbar (for 2004 and 2005), drawn as in Fig. 7. (In 2003 there were not enough float observations to draw geopotential anomaly maps.) Three red rectangles in the lowermost panel indicate the regions of averaging in Fig. 13.

tion. That is, each mode of STMW is thought to be formed in a different anticyclonic circulation in late winter. In May, most of the 17.1°–17.3°C (17.5°–17.7°C) STMW is observed east (west) of 157°E, at which longitude the trough of the KE exists in January–April (Fig. 2). Such STMW distributions probably result from the formation of the 17.1°–17.3°C (17.5°–17.7°C) STMW in a circulation located east (west) of the trough.

The observed/inferred formation and circulation patterns of STMW seem to be well reproduced in the high-resolution numerical model of Rainville *et al.* (2007). In their model, STMW is formed in several anticyclonic circulations just under the crests of the Kuroshio/KE meander, follows each circulation, and gradually escapes from the circulations, mainly toward the south. Complementary use of the Argo float data and such numerical models in the future would lead to the clarification of more detailed variations of STMW and their mechanisms.

5. Interannual Variation of STMW Properties in 2003–2006

In 2005 and the preceding years, there are fewer float data, which are distributed more unevenly in space with decreasing time, especially before April 2004 when the KESS project started deploying floats intensively in the STMW distribution region (Fig. 8). These insufficient data mean that it is somewhat difficult to examine detailed distributions of STMW properties, particularly that of the thickness showing small-scale structure (Fig. 5). The other STMW properties, such as the core θ and S, have large spatial scales and are easier to investigate.

In January–March of 2003–2005, thick STMW is formed between the Kuroshio/KE and ~28°N, as in the same months of 2006 (Fig. 9). After April in each year this thick part stays in a similar latitude range to the winter months, gradually losing its thickness as the season progresses. (The thick part seems to shift southward by three degrees of latitude from July–September to October–December in 2005, but this is probably due to the observation gaps near 31°N, 144° and 152°E in the latter months (Fig. 8).) In the non-outcropping region south of 28°N, STMW is mostly thinner than 150 dbar throughout 2003–2005, as in 2006, producing the stationary front of STMW thickness at ~28°N. Thus, the STMW circulation observed in 2006, characterized by the stagnant pool of thick STMW formed in late winter in the recirculation gyre and the southwestward flow of relatively thin STMW seeping from the thick pool, seems to apply to 2003–2005 on a large scale.

While the southern end of the STMW formation region is located at ~28°N every year, the latitude at which the thickest STMW is formed is different between years. It is at 34°N in 2003 and 2004, while it is located farther south at 31°–32°N in 2005 and 2006. This change is

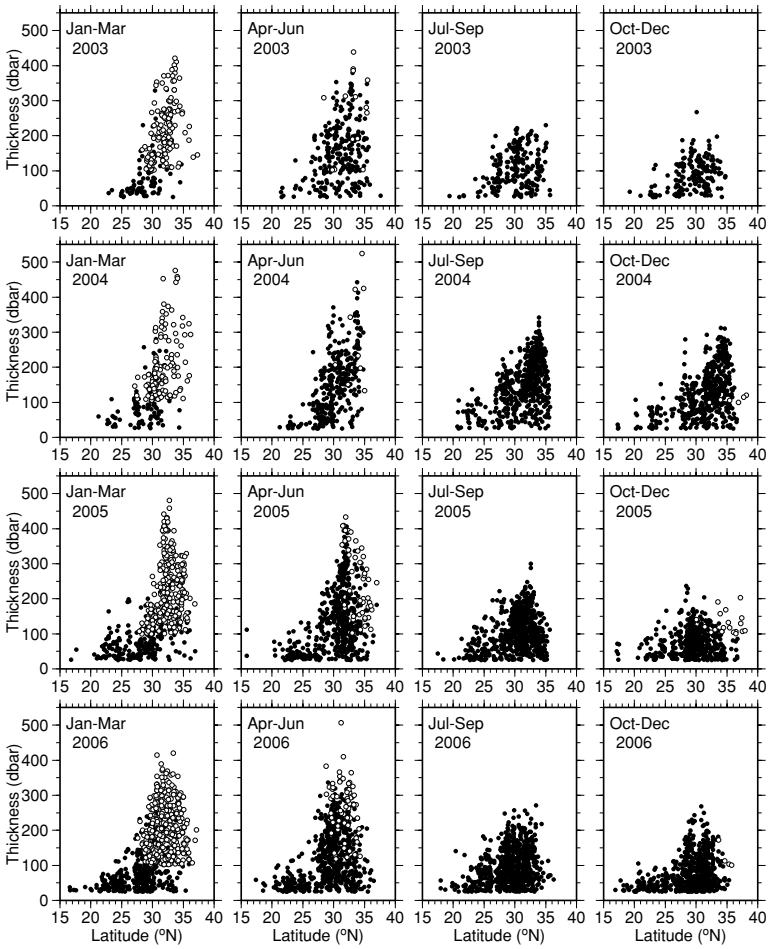

Fig. 9. Plots of STMW thickness against latitude from January–March through October–December of 2003–2006. Open (closed) circles denote outcropping (non-outcropping) STMW.

mainly due to the change in position of the KE recirculation gyre southeast of Japan between about 140° and 155°E (Fig. 10). In 2003 and 2004, the KE is in a stable state, showing two quasi-stationary crests at 144°E and 150°E (Qiu and Chen, 2006), and is accompanied by anticyclonic circulations just south of the crests. At 34°N in these circulations where the permanent thermocline is deep, the thickest STMW is considered to be formed. In 2005, the KE transits to a variable state (Qiu *et al*., 2007), and cyclonic eddies detached from the KE occupy the region just south of the KE, pushing the anticyclonic circulations southward. In 2006, the KE takes a southerly path, likely blocked by cyclonic eddies near 146°E, resulting in the southerly positions of anticyclonic circulations. Accordingly, the thickest STMW is formed at the southerly locations in the latter two years.

Zonal distribution of the core θ of thick STMW formed in late winter 2003–2005 exhibits a feature that is not observed in 2006 (Fig. 11). In each of the three years, the core θ drops eastward by 1.5°C across 140°E, while it decreases much more gradually east of 140°E. This drop is also likely to be related to the distributions of the anticyclonic circulations in the recirculation gyre. The anticyclonic circulations just south of the Kuroshio/KE clearly separate across 140°E, not only in winter 2005 when the Kuroshio takes a large-meander path south of Japan but also in winter 2003 and 2004 when it takes a non-large-meander path, implying that the warmer (colder) STMW is formed in the circulation west (east) of that longitude (Fig. 10). On the other hand, the circulation is continuous across 140°E in 2006, leading to the STMW formation near 140°E and the continuous decrease of the core θ there. The zonal jump across 140°E in 2003–2005 is also seen in the core S and σ_θ distributions (Fig. 11). The STMW formed south of Japan in these years is warmer by 1.5°C, more saline by 0.05–0.1, and less dense by 0.3 kg m^{-3} than that formed east of 140°E.

The core properties east of 140°E exhibit coherent

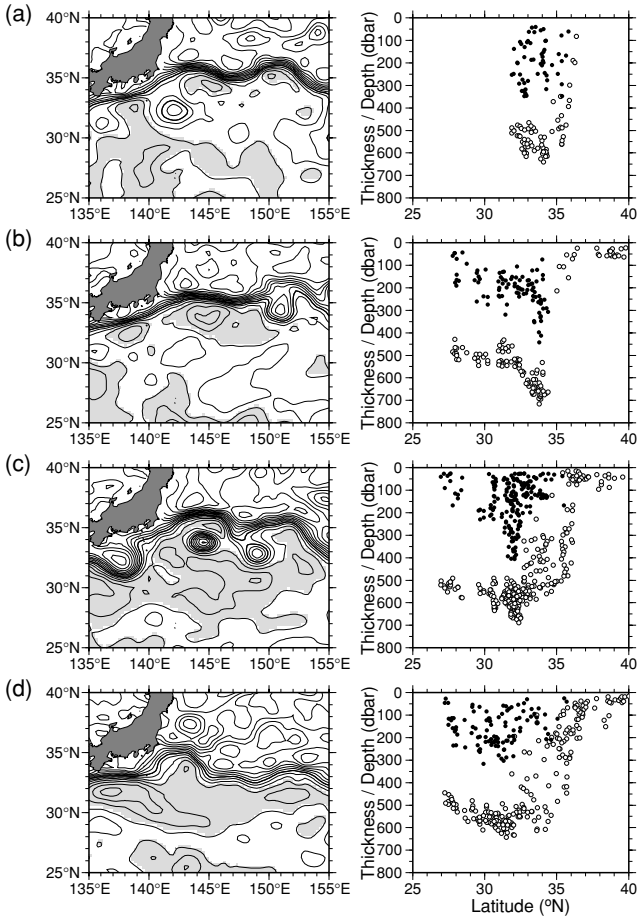

Fig. 10. Altimetric sea surface height maps southeast of Japan in February and March, drawn as in Fig. 7 (left panels) and plots of non-outcropping STMW thickness (closed circles) and the 12°C isotherm depth representing the permanent thermocline depth (open circles) against latitude between 141° and 147°E in April–June (right panels) in (a) 2003, (b) 2004, (c) 2005, and (d) 2006.

interannual variations. The core θ increases from 2003 (16.5°–17.0°C) to 2006 (17.1°–18.2°C) by about 1°C, if we neglect local high/low values. The core S also increases from 2003 (34.71–34.79) to 2005 (34.77–34.87) by about 0.05, remaining high in 2006. This increase is possibly related to a recent salinity increase in the North Pacific Tropical Water (Cannon, 1966), which is the main source of salt in the North Pacific subtropical gyre. Hayashi *et al*. (2005), using T–S data from the repeat section along 137°E, reported that the maximum salinity of the Tropical Water observed at about 10°–16°N increases from 1999 (~34.9) to 2004 (~35.1) by about 0.2. The core σ_θ decreases from 2003 (25.30–25.45 kg m^{-3}) to 2006 (25.10–25.35 kg m^{-3}) by about 0.15 kg m^{-3}, reflecting mainly the increase of the core θ.

Unlike the cases of the core properties, it is difficult to assess the interannual variation of STMW thickness. The maximum thickness in spring is observed between 140° and 150°E every year, being largest in 2004 (442 dbar), second largest in 2005 (406 dbar), third largest in 2003 (379 dbar), and smallest in 2006 (336 dbar). However, Fig. 10 strongly suggests that the thickest STMW is formed locally where the permanent thermocline is particularly deep, and therefore the maximum thickness in each year may not reflect the thickness over a large area. In addition, as mentioned earlier, the float observations before 2006 are neither dense nor uniform enough to resolve such small-scale structure of STMW thickness. For example, the paucity of STMW thinner than 100 dbar between 140° and 150°E in spring 2004 (Fig. 11) is likely because the KESS floats are concentrated within the anticyclonic circulation south of the semi-permanent crest of the KE at 144°E (see figure 2 of Qiu *et al*., 2006).

With an understanding of these limitations, we averaged STMW thickness in the recirculation gyre in each longitudinal range (Fig. 12). At 140°–150°E, the thickness is large in 2003 and 2004 and small in 2005 and 2006, with a significant decrease from 2004 to 2005, which agrees with the result of Qiu at al. (2007). The thickness shows a similar change at 160°–170°E, but not at 150°–160°E in between. The thickness at 150°–160°E increases conversely from 2004 to 2005, being thickest in 2005. Thus, as far as the float data during 2003–2006 are concerned, interannual variation of STMW thickness is different among regions. Again, this is a crude estimate; we need at least several more years of data from the profiling float array comparable to that in 2006, to more properly assess the interannual variation of STMW thickness.

To what degree is the year-to-year change of the core properties detected in the southern, downstream region? Figure 13 shows the time series of core θ during 2003–2006 in three boxes south of the formation region, where STMW never outcrops at the sea surface in winter (see the lowermost panel of Fig. 8 for the box locations). The eastern box at 23°–26°N, 155°–165°E is expected to capture STMW originating in the eastern part of the formation region east of ~160°E, according to the geopotential anomaly maps (e.g., Fig. 8). In this box the core θ steadily increases from the end of 2003 through the end of 2006 (Fig. 13(a)), clearly reflecting the core θ increase in the formation region presented in Fig. 11. Note that the core θ of 17.1°–17.5°C, which characterizes STMW formed at 160°–170°E in winter 2005 (but not that formed in winter 2003 and 2004, which has lower core θ), starts to become apparent in the box in August 2005. This implies that the STMW with the core θ of 17.1°–17.5°C is transported from the formation region to the box in about a half year. The southern end of the formation region at

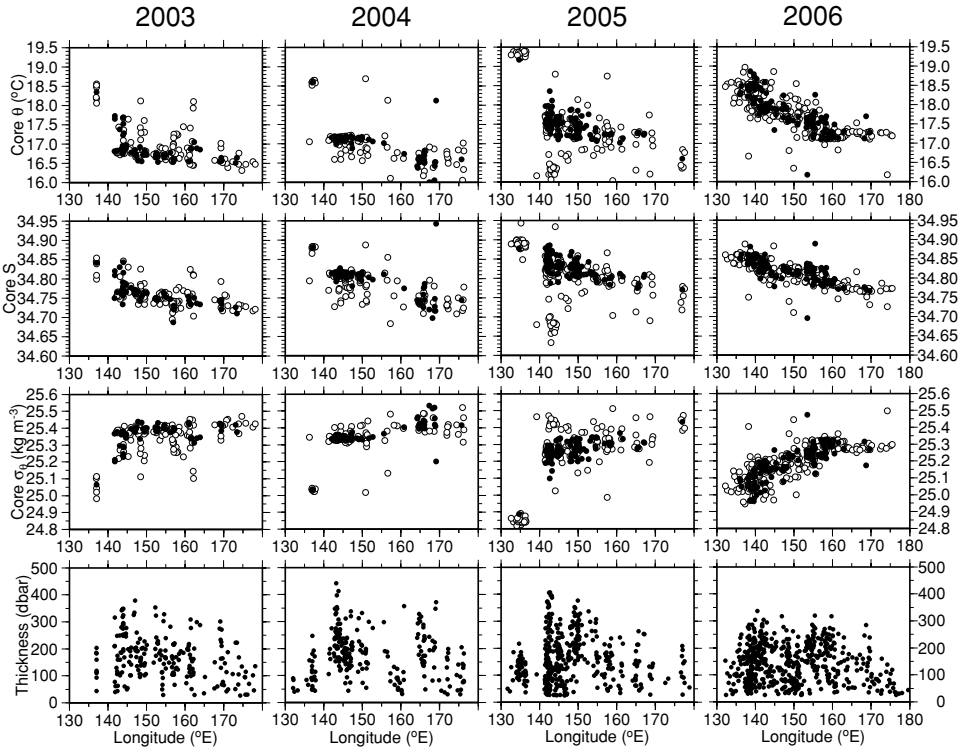

Fig. 11. Plots of θ (top panels), S (second top panels), σ_θ (third top panels) at the core and thickness (bottom panels) against longitude for non-outcropping STMW north of 28°N in April–June from 2003 through 2006. Plots of the core properties were drawn only for STMW thicker than 100 dbar, with closed (open) circles for STMW thicker than 200 dbar (with thickness 100–200 dbar).

~28°N and the northern boundary of the box at 26°N are separated by 2° in latitude. If we roughly estimate the southward component of subsurface flow between the two regions by dividing the zonal gradient of geopotential anomaly shown in Fig. 8 by the Coriolis parameter at 27°N, we obtain

$$\frac{1\,\mathrm{m^2 s^{-2}}}{1.5\times10^{6}\,\mathrm{m}\times6.6\times10^{-5}\,\mathrm{s^{-1}}}=0.01\,\mathrm{m\,s^{-1}}. \qquad (3)$$

Dividing the distance between the two regions by this flow speed yields an advection time of eight months, which is consistent with the observed advection time of a half year.

The middle box at 23°–26°N, 135°–140°E is expected to be fed by various parts of the zonally-elongated STMW formation region. In this box, relatively high core θ is observed from late winter to early summer each year: 17.8°–18.4°C in April–August 2003, 18.4°–18.7°C in April–July 2004, 19.4°C in May 2005, and 18.5°–19.0°C in February–March 2006 (Fig. 13(b)). Each of these core θ values coincides with that of STMW originating in the westernmost part of the formation region west of 140°E in the same year (Fig. 11), implying that warm STMW formed south of Japan is quickly transported southward every year. Except for these high values, the core θ in the box increases gradually from the end of 2003 through the end of 2006, presumably reflecting the core θ increase in the formation region east of 140°E with various time lags longer than about a half year.

The core θ increase is observable even in the western box at 22°–26°N, 122°–127°E just east of Taiwan, although the data represent only the last 2.5 years there (Fig. 13(c)). The box exhibits high core θ of 18.5°–18.8°C from September 2004 through January 2005 and the other core θ increasing for 2.5 years, probably associated with the STMW originating west and east of 140°E in the formation region, respectively. A comparison of this core θ variation with that in the middle box suggests that the STMW observed in the western box is advected from near the middle box in about 3–5 months.

The increase of the core S in the formation region from 2003 through 2005 presented in Fig. 11 is also clearly detected in the three boxes (not shown). Thus, the float data for four years clearly demonstrate that STMW transports the property anomalies from the formation region to the western boundary. In the present study, however, we could not examine in detail how the property anoma-

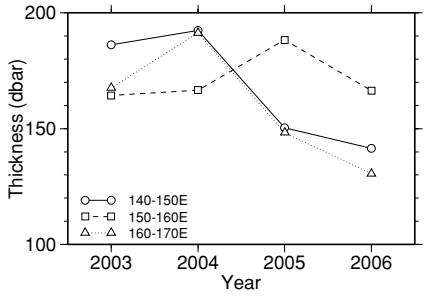

Fig. 12. Time series of STMW thickness in May and June, averaged north of 28°N, between 140° and 150°E (solid curve with circles), 150° and 160°E (dashed curve with squares), and 160° and 170°E (dashed curve with triangles). The thickness only at float observation points where the 12°C isotherm is deeper than 475, 450, and 425 dbar, respectively, was averaged, first in each 1° square and then in each area spanning 10° in longitude.

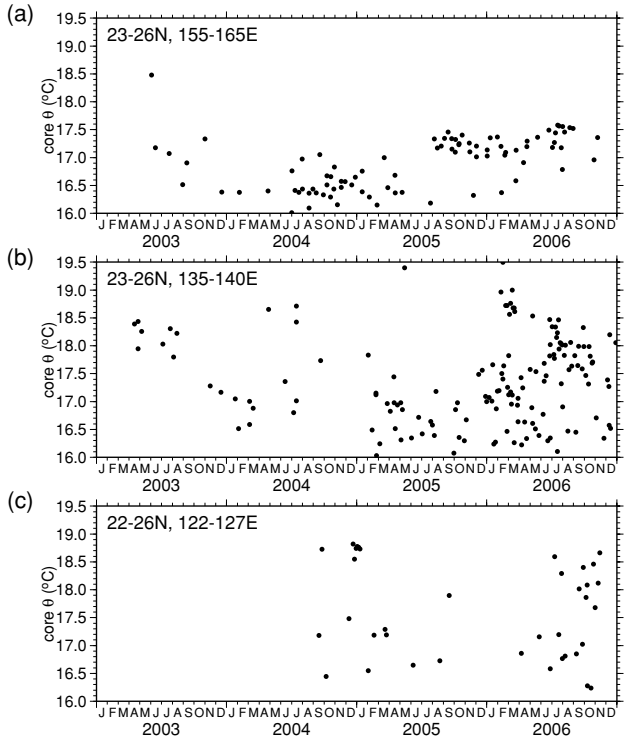

Fig. 13. Time series of the core θ of STMW observed in (a) 23°–26°N, 155°–165°E, (b) 23°–26°N, 135°–140°E, and (c) 22°–26°N, 122°–127°E.

lies produced in various parts of the formation region reach a given area in the downstream region with different time lags, due to brevity of the data and the inadequate data density in the southern region. In several years, using longer time-series float data and complementary high-resolution numerical models, we shall be able to examine quantitatively how these anomalies accumulate in the downstream region, changing the oceanic structure and flow field there.

6. Summary and Discussion

Temperature and salinity data during 2003–2006 from Argo profiling floats have been analyzed to examine the formation and circulation of STMW and interannual variation of its properties. In 2006, thick STMW is formed in late winter in the zonally-elongated recirculation gyre south of the Kuroshio/KE, which extends north of ~28°N, from 135°E to near the date line. The recirculation gyre consists of several anticyclonic circulations, in each of which STMW is formed with a characteristic θ. After spring, the thick STMW, while gradually decreasing its thickness, tends to be continually trapped in the respective circulations, remaining in the formation region. From this stagnant pool of thick STMW, some portion seeps little by little into the southern region, where the southwestward subsurface current advects relatively thin STMW as far as 20°N to the south and just east of Taiwan to the west. Such STMW circulation seems to apply to the other years, 2003–2005.

The thick STMW just after the formation in each year becomes colder, less saline, and denser to the east, with a jump of the core properties across 140°E in 2003–2005. In these three years, the STMW formed in the anticyclonic circulation south of Japan near 135°E is warmer by 1.5°C, more saline by 0.05–0.1, and less dense by 0.3 kg m^{-3} than that formed in the anticyclonic circulations east of 140°E, regardless of whether the Kuroshio south of Japan takes a large-meander path or a non-large-meander path. This jump is not observed in 2006, when the KE takes a southerly path southeast of Japan and the anticyclonic circulation is continuous across 140°E. East of 140°E, the core properties of the thick STMW gradually change zonally every year, and show coherent interannual variations. The core θ increases from 2003 through 2006 by about 1°C, and the core S also increases from 2003 through 2005 by about 0.05, remaining high in 2006. These changes are clearly detected in the downstream region south of the recirculation gyre where STMW is never ventilated in winter, as far downstream as just east of Taiwan, with reasonable time lags.

Since the interannual variation of core θ is expected to be related to that of the winter cooling in the STMW formation region, we averaged net surface heat flux at 29°–36°N, 142°–160°E from October through March each year, using daily mean reanalysis data of the National Centers for Environment Prediction and the National Center for Atmospheric Research (NCEP/NCAR; Kistler *et al*., 2001). The average heat flux from the ocean to the atmosphere is largest in 2002/03 (280 W m^{-2}), second

largest in 2005/06 (256 W m^{-2}), third in 2003/04 (252 W m^{-2}), and smallest in 2004/05 (247 W m^{-2}), showing a weakly decreasing trend. There is also a suggestion that the interannual variation of core θ is related to that of the transport of the Kuroshio that brings warm surface water to the STMW formation region (Yasuda and Hanawa, 1997; Hanawa and Kamada, 2001). The one-year moving average of the Kuroshio transport in the East China Sea, estimated using sea-level data and the regression equation of Kawabe (1995), steadily increases from 24×10^6 $m^3 s^{-1}$ in winter 2002/03 to 27×10^6 $m^3 s^{-1}$ in winter 2005/06 (M. Kawabe, personal communication). Thus, the trends in both the surface heat flux and the Kuroshio transport during the four years, particularly the latter, are consistent with the increasing trend of the core θ.

The present study has demonstrated that the existence and state of the recirculation gyre of the Kuroshio/KE are essential in the formation and circulation of STMW and in determining the distribution of its properties. The state of the recirculation gyre also affects the interannual variation of STMW thickness, through the associated cyclonic eddies carrying high potential-vorticity KE water into the gyre (Qiu and Chen, 2006). The relation of the STMW variation to the state of the recirculation gyre, as well as the other factors, needs further comprehensive examination, using more data from the Argo float array that has just been completed.

Acknowledgements

The author thanks Tsuyoshi Ohira for help in preparing the Argo float data, Shigeki Hosoda for advice on the optimal interpolation technique, and Toshio Suga, Masami Nonaka, Bo Qiu, and an anonymous reviewer for helpful comments. The Argo float data used in this study were collected and made freely available by the International Argo Project and the national programs that contribute to it (http://www.argo.ucsd.edu, http://argo.jcommops.org). Argo is a pilot program of the Global Ocean Observing System.

References

Akima, H. (1970): A new method of interpolation and smooth curve fitting based on local procedures. *J. Assoc. Comput. Math.*, **17**, 589–602.

Argo Science Team (2001): Argo: The global array of profiling floats. p. 248–258. In *Observing the Oceans in the 21st Century*, ed. by C. J. Koblinsky and N. R. Smith, GODAE Project Office, Bureau of Meteorology, Melbourne.

Bingham, F. M. (1992): Formation and spreading of Subtropical Mode Water in the North Pacific. *J. Geophys. Res.*, **97**, 11177–11189.

Bretherton, F. P., R. E. Davis and C. B. Fandry (1976): A technique for objective analysis and design of oceanographic experiment applied to MODE-73. *Deep-Sea Res.*, **23**, 559–582.

Cannon, G. A. (1966): Tropical waters in the western Pacific Oceans, August–September 1957. *Deep-Sea Res.*, **13**, 1139–1148.

Conkright, M. E., R. A. Locarnini, H. E. Garcia, T. D. O'Brien, T. P. Boyer, C. Stephens and J. I. Antonov (2002): World Ocean Atlas 2001: Objective Analysis, Data Statistics, and Figures, CD-ROM Documentation. National Oceanographic Data Center, Silver Spring, MD, 17 pp.

Ducet, N., P. Y. Le Traon and G. Reverdin (2000): Global high-resolution mapping of ocean circulation from TOPEX/Poseidon and ERS-1 and -2. *J. Geophys. Res.*, **105**, 19477–19498.

Ebuchi, N. and K. Hanawa (2001): Trajectory of mesoscale eddies in the Kuroshio recirculation region. *J. Oceanogr.*, **57**, 471–480.

Hanawa, K. (1987): Interannual variations of the winter-time outcrop area of Subtropical Mode Water in the western North Pacific Ocean. *Atmos. Ocean*, **25**, 358–374.

Hanawa, K. and J. Kamada (2001): Variability of core layer temperature (CLT) of the North Pacific Subtropical Mode Water. *Geophys. Res. Lett.*, **28**, 2229–2232.

Hanawa, K. and L. D. Talley (2001): Mode waters. p. 373–386. In *Ocean Circulation and Climate*, ed. by J. Church *et al.*, Academic Press, London.

Hanawa, K. and H. Yoritaka (2001): North Pacific Subtropical Mode Waters observed in long XBT cross sections along 32.5°N line. *J. Oceanogr.*, **57**, 679–692.

Hayashi, K., T. Soga, Y. Takatsuki and K. Ishikawa (2005): Salinity increasing trend of the North Pacific Tropical Water in recent years. p. 278. In *Abstracts of 2005 Spring Meeting of Oceanogr. Soc. Japan*, Tokyo Univ. Mar. Sci. Tech., Tokyo (in Japanese).

Japan Meteorological Agency (2005): Data Report of Oceanographic and Marine Meteorological Observations. No. 94.

Japan Meteorological Agency (2006): Data Report of Oceanographic and Marine Meteorological Observations. No. 95.

Kawabe, M. (1995): Variations of current path, velocity, and volume transport of the Kuroshio in relation with the large meander. *J. Phys. Oceanogr.*, **25**, 3103–3117.

Kawai, H. (1972): Hydrography of the Kuroshio Extension. p. 235–352. In *Kuroshio—Its Physical Aspects*, ed. by H. Stommel and K. Yoshida, Univ. Tokyo Press, Tokyo.

Kistler, R., E. Kalnay, W. Collins, S. Saha, G. White, J. Woollen, M. Chelliah, W. Ebisuzaki, M. Kanamitsu, V. Kousky, H. van den Dool, R. Jenne and M. Fiorino (2001): The NCEP-NCAR 50-Year Reanalysis: Monthly Means CD-ROM and Documentation. *Bull. Amer. Meteor. Soc.*, **82**, 247–268.

Kubokawa, A. (1999): Ventilated thermocline strongly affected by a deep mixed layer: A theory for subtropical countercurrent. *J. Phys. Oceanogr.*, **29**, 1314–1333.

Kubokawa, A. and T. Inui (1999): Subtropical countercurrent in an idealized ocean GCM. *J. Phys. Oceanogr.*, **29**, 1303–1313.

Kuragano, T. and M. Kamachi (2000): Global statistical space-time scales of oceanic variability estimated from the TOPEX/POSEIDON altimeter data. *J. Geophys. Res.*, **105**, 955–974.

Kwon, Y.-O. and S. C. Riser (2004): North Atlantic Subtropical Mode Water: A history of ocean-atmosphere interaction 1961–2000. *Geophys. Res. Lett.*, **31**, L19307, doi:10.1029/2004GL021116.

Masuzawa, J. (1969): Subtropical Mode Water. *Deep-Sea Res.*, **16**, 463–472.

Mizuno, K. and W. B. White (1983): Annual and interannual variability in the Kuroshio Current System. *J. Phys. Oceanogr.*, **13**, 1847–1867.

Nishikawa, S. and A. Kubokawa (2007): Mixed layer depth front and subduction of low potential vorticity water in an idealized ocean GCM. *J. Oceanogr.*, **63**, 125–134.

Oka, E. and T. Suga (2003): Formation region of North Pacific subtropical mode water in the late winter of 2003. *Geophys. Res. Lett.*, **30**, 2205, doi:10.1029/2003GL018581.

Oka, E., T. Suga and L. D. Talley (2007): Temporal variability of winter mixed layer in the mid- to high-latitude North Pacific. *J. Oceanogr.*, **63**, 293–307.

Qiu, B. (2002): The Kuroshio Extension system: Its large-scale variability and role in the midlatitude ocean-atmosphere interaction. *J. Oceanogr.*, **58**, 57–75.

Qiu, B. and S. Chen (2005): Variability of the Kuroshio Extension jet, recirculation gyre and mesoscale eddies on decadal timescales. *J. Phys. Oceanogr.*, **35**, 2090–2103.

Qiu, B. and S. Chen (2006): Decadal variability in the formation of the North Pacific Subtropical Mode Water: Oceanic versus atmospheric control. *J. Phys. Oceanogr.*, **36**, 1365–1380.

Qiu, B., P. Hacker, S. Chen, K. A. Donohue, D. R. Watts, H. Mitsudera, N. G. Hogg and S. R. Jayne (2006): Observations of the Subtropical Mode Water evolution from the Kuroshio Extension System Study. *J. Phys. Oceanogr.*, **36**, 457–473.

Qiu, B., S. Chen and P. Hacker (2007): Effect of mesoscale eddies on subtropical mode water variability from the Kuroshio Extension System Study (KESS). *J. Phys. Oceanogr.*, **37**, 982–1000.

Rainville, L., S. R. Jayne, J. L. McClean and M. E. Maltrud (2007): Formation of subtropical mode water in a high-resolution ocean simulation of the Kuroshio Extension region. *Ocean Modell.*, **17**, 338–356.

Roemmich, D., J. Gilson, R. Davis, P. Sutton, S. Wijffels and S. Riser (2007): Decadal spinup of the South Pacific subtropical gyre. *J. Phys. Oceanogr.*, **37**, 162–173.

Suga, T. and K. Hanawa (1990): The mixed layer climatology in the northwestern part of the North Pacific subtropical gyre and the formation area of Subtropical Mode Water. *J. Mar. Res.*, **48**, 543–566.

Suga, T. and K. Hanawa (1995a): The subtropical mode water circulation in the North Pacific. *J. Phys. Oceanogr.*, **25**, 958–970.

Suga, T. and K. Hanawa (1995b): Interannual variations of North Pacific Subtropical Mode Water in the 137°E section. *J. Phys. Oceanogr.*, **25**, 1012–1017.

Suga, T., K. Hanawa and Y. Toba (1989): Subtropical mode water in the 137°E section. *J. Phys. Oceanogr.*, **19**, 1605–1618.

Suga, T., K. Motoki, Y. Aoki and A. M. Macdonald (2004): The North Pacific climatology of winter mixed layer and mode waters. *J. Phys. Oceanogr.*, **34**, 3–22.

Sugimoto, S. and K. Hanawa (2005): Remote reemergence areas of winter sea surface temperature anomalies in the North Pacific. *Geophys. Res. Lett.*, **32**, L01606, doi:10.1029/2004GL021410.

Taneda, T., T. Suga and K. Hanawa (2000): Subtropical mode water variation in the southwestern part of the North Pacific subtropical gyre. *J. Geophys. Res.*, **105**, 19591–19598.

Uehara, H., T. Suga, K. Hanawa and N. Shikama (2003): A role of eddies in formation and transport of North Pacific Subtropical Mode Water. *Geophys. Res. Lett.*, **30**, 1705, doi:10.1029/2003GL017542.

Yasuda, T. and K. Hanawa (1997): Decadal changes in the mode waters in the midlatitude North Pacific. *J. Phys. Oceanogr.*, **27**, 858–870.

Yasuda, T. and K. Hanawa (1999): Composite analysis of North Pacific subtropical mode water properties with respect to the strength of the wintertime East Asian monsoon. *J. Oceanogr.*, **55**, 531–541.